

Influence of along-shore advection and upwelling on coastal temperature at Kaikoura Peninsula, New Zealand

STEPHEN M. CHISWELL

National Institute of Water & Atmospheric
Research Ltd
P. O. Box 14 901
Wellington, New Zealand
email: s.chiswell@niwa.cri.nz

DAVID R. SCHIEL

Marine Ecology Research Group
Zoology Department
University of Canterbury
Private Bag 4800
Christchurch, New Zealand

Abstract Thermistor data from around Kaikoura Peninsula, New Zealand, show that in the synoptic band, temperature fluctuations at 1 m are coherent with the along-shore wind with a 90° phase difference. At 5 m, however, the coherence is not as high, and the phase relationship is in the opposite sense. Along this coast, wind-driven advection of the coastal current and upwelling have opposite effects on temperature. A simple model is developed which has along-shore advection and upwelling terms parameterised in terms of the wind and two unknown coefficients. Solving for the coefficients shows that at 1 m, temperature variability is determined by along-shore advection, whereas at 5 m, temperature variability is determined principally by upwelling.

Keywords oceanography; temperature; coastal communities; upwelling

INTRODUCTION

It is well known both in New Zealand (Andrew 1988; Creese 1988; Jones 1988; Schiel 1988) and elsewhere (e.g., Underwood & Fairweather 1989; Menge et al. 1999) that predators and grazers can affect the structure of sessile invertebrate and macrophyte populations, and that such processes can vary considerably on a localised scale.

However, physical processes within the offshore environment can also affect the recruitment of organisms and productivity on rocky coasts, and may account for variation among sites (Gaines & Roughgarden 1985; Underwood & Fairweather 1989; Menge 1992). An example of such a process is upwelling, which may bring nutrients into the coastal zone and also isolate coastal surface waters from oceanic waters. For example, Farrell et al. (1991) found that barnacle larvae in central California were brought inshore during times when there was a relaxation of along-shore winds and a cessation in upwelling. They found alternating periods of onshore and offshore transport of the surface water layer over a period of a few weeks during spring and summer. Other studies in central California have shown a good correlation between larval abundance, settlement, and recruitment of intertidal organisms (Gaines & Roughgarden 1985). These processes may account for some of the differences in rocky shore populations between the east and west coast of the South Island of New Zealand (Menge et al. 1999).

Ecological studies around the Kaikoura Peninsula, South Island, have found significant variation among intertidal sites in the recruitment and growth of macrophytes (Ramage & Schiel 1999; Schiel & Taylor 1999). We hypothesised that some of this variation was because of differences in the character of the water mass around the peninsula, particularly as it influences inshore reefs, and that similar processes to those happening off California may be important near Kaikoura Peninsula.

With predominantly south-westerly winds, the east coast of the South Island is generally a

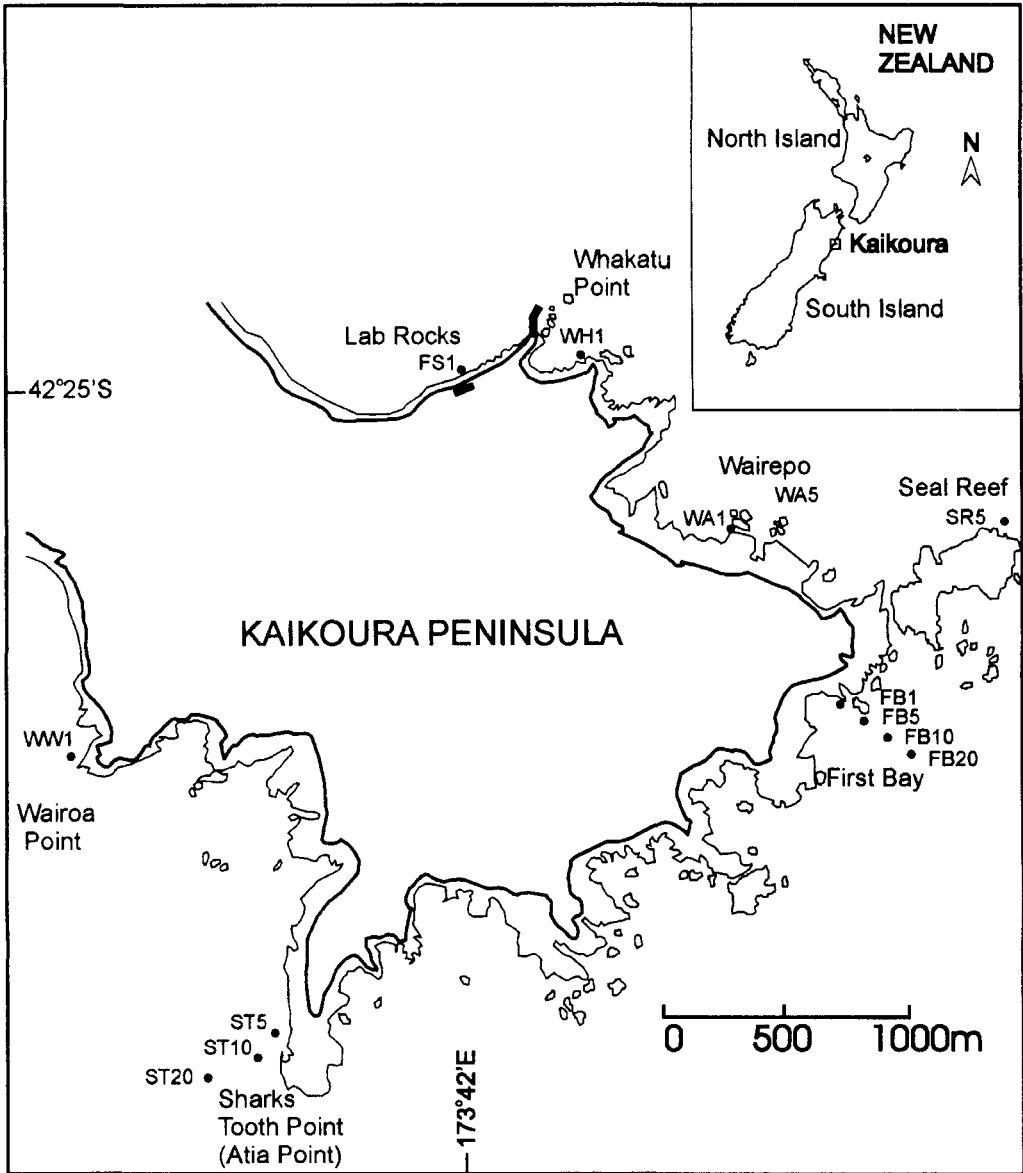


Fig. 1 Map of Kaikoura Peninsula, New Zealand, showing thermistor locations. Codes indicate site names: FS = Field Station, WH = Whakatu Point, WA = Wairepo Flats, FB = First Bay, ST = Sharks Tooth Point, SR = Seal Reef, and WW = Wairoa Point. Depth (m) of thermistors is designated by the number after the location code. Fine line around the peninsula indicates the position of the reefs exposed at low tide. Scale is in metres.

downwelling coast. During northerly winds, there may be a cessation of downwelling, or even upwelling, which could bring deep nutrient-rich waters into the coastal zone. There is at least one documented case of northerly winds inducing upwelling off Kaikoura (Heath 1972).

The coastal current flowing north-eastwards past the Kaikoura Peninsula is the Southland Current, fluctuations in which are known to be strongly wind driven (Chiswell 1996). Temperatures within the Southland Current decrease to the south, so that increased transport in the Southland Current, usually

associated with increased southerly winds, leads to a drop in coastal sea surface temperature. Such an event was observed by Heath (1970) who recorded a rapid decrease in temperature off Kaikoura following a severe southerly storm.

Therefore, southerly winds can lead to a drop in temperature because of acceleration of the Southland Current, whereas northerly winds can decrease temperature because of upwelling. Thus the two effects of along-shore advection and upwelling work in opposition along this coast, and temperature variability is unlikely to be simply related to fluctuations in wind stress. To understand these processes better around Kaikoura Peninsula, we deployed temperature thermistors in late 1997 at several depths around the peninsula.

In this article, we use wind records from Kaikoura to investigate the competing roles of upwelling/downwelling and along-shore advection on water temperature around the peninsula. We show that that in the synoptic band (i.e., where temperature is controlled by weather events), temperature fluctuations at 1 m are coherent with the along-shore wind with a 90° phase difference. At 5 m, however, the coherence is not as high, and the phase relationship is in the opposite sense. We use these findings to derive a simple model which has along-shore advection and upwelling/downwelling parameterised in terms of the along-shore wind and two unknown coefficients.

REGIONAL HYDROGRAPHY

Several different water masses are thought to be potentially important in the region. The waters inshore are those of the Southland Current. Water within the Southland Current is mainly subtropical water (STW), mixed with some Australasian subantarctic water (Houtman 1964), and it has generally been suggested that the source of the current is water from the Subtropical Front (STF) west of New Zealand. This view was corroborated by Heath (1975).

The Southland Current is bounded to the east by low salinity subantarctic water (SAW), and differences in both temperature and salinity between the inshore and offshore waters are sufficiently large to form a sharply delineated front, known locally as the Southland Front.

Although the mean currents in the region are thought to be from the south, it is also known that

there is some variability in the flows, and it may be that on occasion Kaikoura is bathed by STW from the north. Recently, Shaw & Vennell (1999) documented "wisps" of SAW intruding across the STF into the Kaikoura region, but whether these waters impact the coastal zone is not known.

METHODS

Thermistor data

Thermistors were deployed at seven sites around the Kaikoura Peninsula (Fig. 1). The sites were chosen principally to obtain reasonable sampling around the peninsula, but because of the variable and occasionally rough sea conditions, the final locations also depended on their ease of access. The southern shore of the peninsula is especially difficult to work from because of exposure to large swells from the south. At most sites, probes were deployed at 1 m depth below chart datum. At some sites, additional thermistors were deployed at 5, 10, and 20 m depths. We denote the thermistor records according to a 2-character location (see Fig. 1) and depth. For example, the 1 m record from directly off the Edward Percival Field Station is denoted as FS1.

Because of data failures, losses of some thermistors, instrument failures, and poor weather preventing instrument turn-around, no sites returned complete records at all depths. The most complete record for 1 m was from FS1. At 5 and 10 m, the most complete records were from FB5 and FB10, respectively.

Temperature probes were from Onset Corporation (Optic StowAway), with a range of -5 to 37°C. Over the central portion of their range, these thermistors are accurate to within 0.1°C (Onset Corporation data). They were set to record temperature at 30-min intervals. Each probe was put into a protective sheath and attached to heavy weights on the sea floor. They were turned around by divers at 3-month intervals, the exact timing depending on sea conditions. Over the course of the year, several probes were lost through cases being broken and others could not be read. In some cases, data were recovered by the manufacturer.

Meteorological data

Wind speed (m s^{-1}), air dry and wet bulb temperatures ($^{\circ}\text{C}$), and radiation (MJ m^{-2}) were obtained from the NIWA climate database. The wind

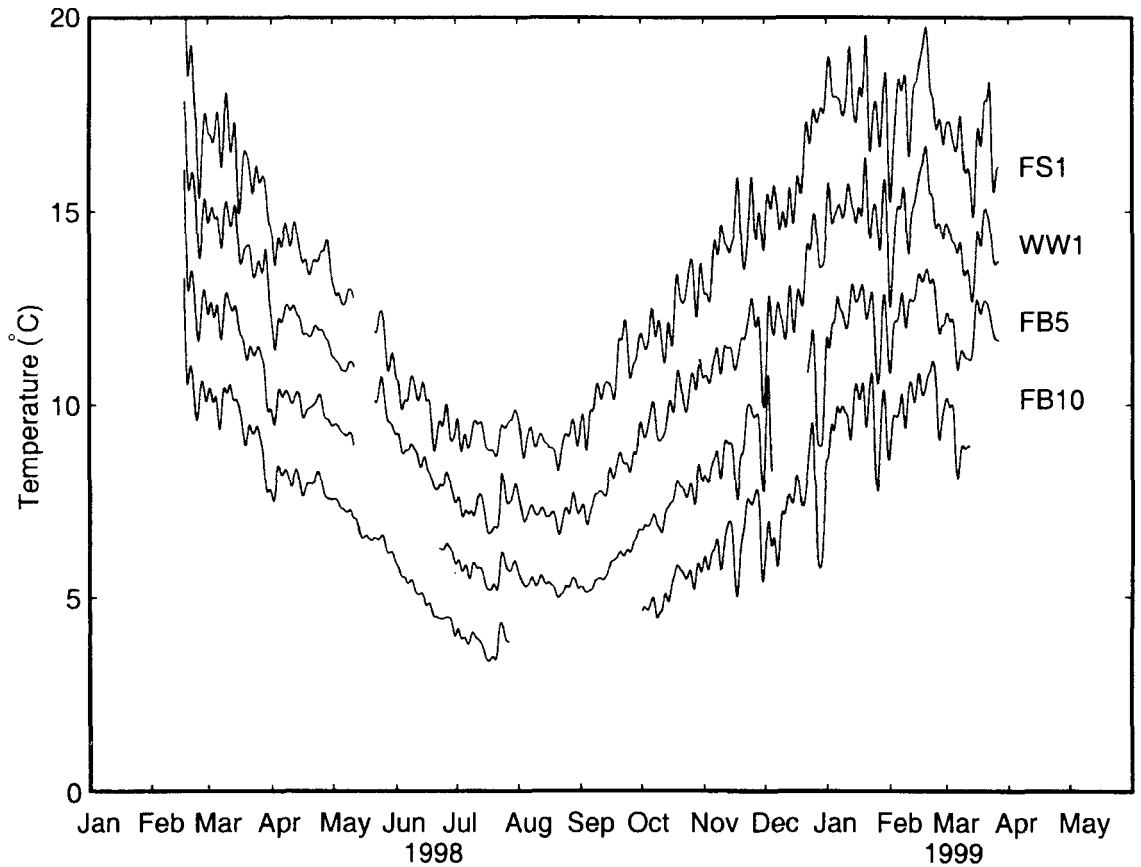


Fig. 2 Four of the temperature records collected around Kaikoura Peninsula, New Zealand. Locations and instrument depths are as indicated in Fig. 1. FS1 has been plotted with no offset, other records have been successively offset by 2°C.

records came from the recording anemometer in the New Zealand Meteorological Service station located at the highest point on the Kaikoura Peninsula. Wind speed and direction were used to obtain wind velocity components. These were then rotated into along-shore and cross-shore directions. The along-shore direction was chosen to maximise the variance in the along-shore wind, and put the along-shore direction at 65° east of north, which is about the same as the orientation of the South Island (i.e., the large-scale topography, rather than the local Kaikoura Peninsula).

Observations

The principal records used in the analysis in are shown in Fig. 2. These records have been low-pass filtered using a Butterworth filter with half-power period of 3 days to remove the diurnal heating signal.

The thermistors were deployed in mid February when temperatures were near the maximum their seasonal maximum. This is consistent with the offshore cycle which shows highest sea surface temperature in February (Chiswell 1994; Uddstrom & Oien 1999).

The annual cycle was removed from records that were long enough to allow a fit. Although the annual cycle is not our main focus, it is of sufficient interest to warrant some discussion. Where the records were long enough, a 365-day period sinusoid was fitted using a least-squares technique, to return amplitude and phase. Three records at 1 m (FS1, WW1, and WA1) returned amplitudes of between 4 and 4.5°C, with the highest temperatures occurring about the first week in February. The two records from 5 m (FB5 and ST5) returned slightly lower amplitudes and a phase retarded by c. 10 days compared to the

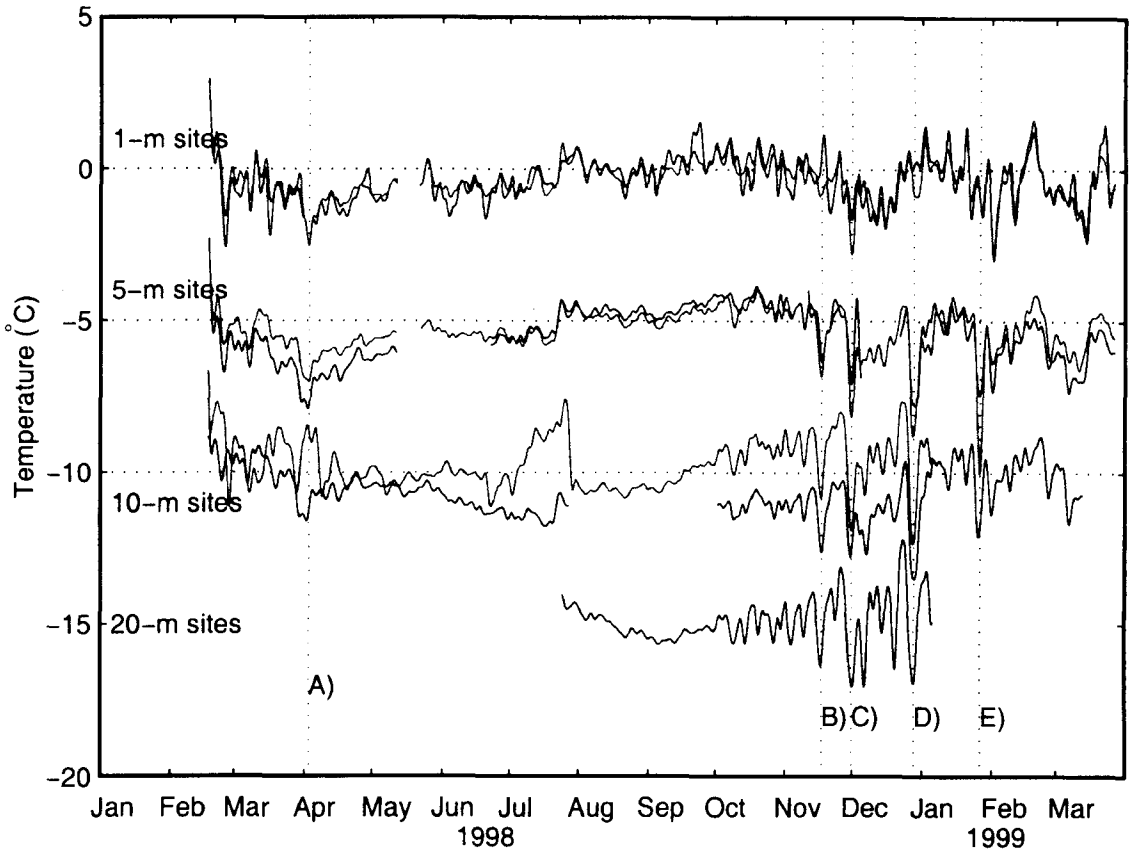


Fig. 3 Detrended temperature. Records have had an annual cycle removed, and have been filtered with a low-pass filter to remove diurnal cycles (see text). Records are displaced according to instrument depth (i.e., 5 m records are displaced by 5°C). Cooling events labelled A–E are discussed in the text.

1 m values. The single record from 10 m (FB10) returned similar values to the 5 m records.

Sites returning nearly a full year of data from 1, 5, 10, and 20 m depths were low-pass filtered and their annual cycles were removed (Fig. 3). Perhaps the most noticeable features of the synoptic band are distinct cooling events superimposed on this low-frequency oscillation. Some of these events, but not all, occurred at all sites. We do not show them here, but histograms of these temperature records confirm cool events were more common than warm events. These events were short-lived, usually lasting only a few days, and in general occurred during the summer. They typically had larger amplitudes at the deeper sites.

We have labelled five cool events (A–E) in Fig. 3. The events are not consistent throughout the records. For example, Event A showed a 1–2°C drop in all

sites, except ST10, whereas Events B and D were much stronger at the deeper sites, showing up to 4°C drop at 5 m depth. In some cases, e.g., Events A and E the events were seen uniformly around the peninsula. Other events (C, D) had larger amplitude on the south side of the peninsula. Even within relatively shore distances around the peninsula, there are differences in the events, e.g., compare the 5-m records at FB and ST.

Figure 4 shows the along-shore wind scaled by an arbitrary constant and superimposed on the temperature record from 5 m (FB5) for the time period covering events D–E. Each of these cooling events was preceded by a relatively strong northerly wind event (negative U), suggesting that they are indeed responses to upwelling. However, it is interesting to note that not all northerly events are followed by cool events (e.g., the wind event on 3

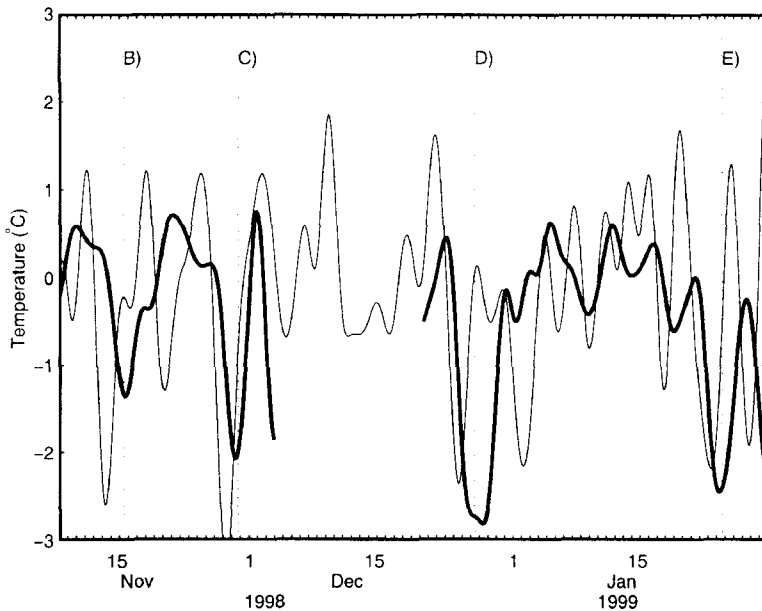


Fig. 4 Along-shore wind velocity (light line) scaled by an arbitrary constant and superimposed on the detrended temperature (solid line) record from 5 m at FB for the time period covering events B–E shown in Fig. 3.

January 1999 was not followed by a temperature drop).

Cross-spectra between the along-shore wind and temperature at 1 m (FS1) and 5 m (FB5) depth were calculated using a weighted overlapped segment method as described by Harris (1978) (Fig. 5). At a depth of 1 m, coherence-squared exceeds the 95% confidence levels at several bands centred near 7 and 5 days, and, even though the records have been low pass filtered, at 1 day. The significant coherence at 1 day does not necessarily suggest a direct link between the wind and temperature, because daily radiative heating will be coherent with diurnal cycles in the wind field. The other peaks in the synoptic band, however, probably indicate a direct influence of the wind forcing on temperature. Cross-spectral phase where coherence-squared exceeds the 95% confidence limits is statistically indistinguishable from 90° . At 5 m, however, there is less coherence between the along-shore wind and temperature, with significant coherence occurring only near 7–8 day periods. Cross-spectral phase is statistically indistinguishable from -90° .

Bearing in mind that differentiation of a timeseries leads to a 90° phase change in its Fourier transform, the coherences shown in Fig. 5 suggest that wind is coherent with the time-derivative of temperature, and this observation leads us to the development of the model discussed in the next section.

Model

If coastal temperature is controlled only by along-shore advection and upwelling (i.e., all other process such as radiative heating and wind mixing are ignored), the rate of change of temperature can be written:

$$\frac{\partial T}{\partial t} = -u \frac{\partial T}{\partial x} - w \frac{\partial T}{\partial z} \quad (1)$$

The co-ordinate system is such that x is along-shore (positive to the north), z is vertical (positive up), u is the along-shore current, w is the vertical velocity. For simplicity, we refer to w as the upwelling velocity, but w is negative for downwelling, i.e., from the model's perspective downwelling is negative upwelling. Temperature within the Southland current increases to the north, and temperature decreases with depth, so that locally both $\partial T/\partial x$ and $\partial T/\partial z$ are positive.

Chiswell (1996) has shown that fluctuations in the Southland Current off Otago were in phase with the Invercargill wind, and can be modelled by convolving the wind velocity with an impulse-response function which is nearly a delta function. This is probably because of the influence of bottom friction. Off Otago observed current showed higher coherence with along-shore wind velocity than with wind-stress calculated assuming a quadratic stress law. Based on Chiswell's earlier result, we model

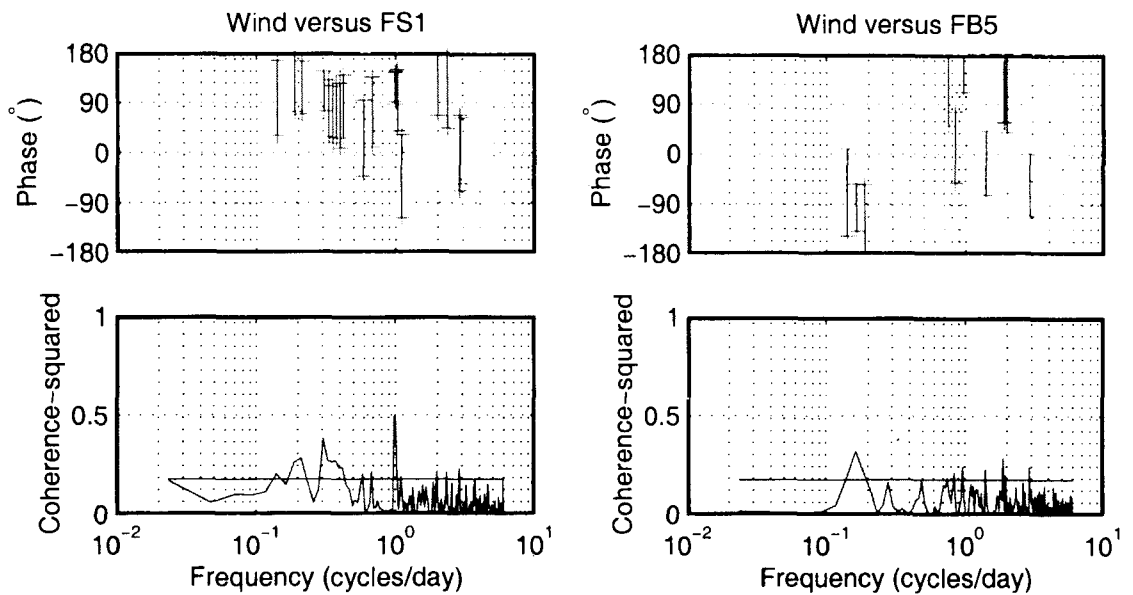


Fig. 5 Cross-spectra between temperature and along-shore wind. Left panels: at 1 m (Site FS1). Right panels: at 5 m (Site FB5). In each case, lower panel shows coherence-squared with 95% confidence limits indicated by the horizontal line. Upper panels show cross-spectral phase where coherence-squared exceeds 95% confidence levels. Vertical bars on phase show the 95% confidence limits.

the along-shore current as proportional to the along-shore wind velocity.

The upwelling velocity w is taken to be proportional to Ekman transport τ/f , where τ is the along-shore wind-stress (Pond & Pickard 1978). Empirical tests not detailed here show a better result is obtained if t is a linear rather than quadratic stress (i.e., $\tau \propto U$).

Thus, the model derived from Equation 1 becomes:

$$\frac{\partial T}{\partial t} = -\alpha U + \beta \frac{\partial T}{\partial z} U \quad (2)$$

where U is the along-shore wind velocity, α and β are fitable parameters; α has dimensions $^{\circ} \text{m}^{-1}$ and β is dimensionless. The first term on the right hand side is the advective term; since $\partial T/\partial x$ is unknown, we have assumed it to be constant, in which case it collapses into α . We denote the second term as the upwelling term—downwelling occurs when this term is negative. Since we can estimate $\partial T/\partial z$, and it has some time dependence (see later) $\partial T/\partial z$ is not incorporated into β . Both α and β are positive so that an increase in U (i.e., a downwelling, southerly wind) leads to a drop in temperature from the advective term, but an increase in temperature from

the upwelling term. It is worth noting here that the absolute values of α and β are unimportant in this analysis because they do not provide much information on the physics involved. Instead, the relative roles of advection to upwelling are given by the dimensionless ratio $\alpha/(\beta \partial T/\partial z)$.

To develop the model, we use the low-passed, but not seasonally detrended, temperature from two depths (1 m and 5 m) to estimate $\partial T/\partial z$. Since no sites returned full records at both these depths, we use the records from FS1 and FB5, denoted as T_1 and T_5 , respectively. This forces us to make the explicit assumption that there are no spatial temperature gradients around the peninsula (this point is treated in the Discussion). The vertical temperature gradient is estimated as $\partial T/\partial z = (T_1 - T_5)/4$, this term is smoothed by using an annual cycle fit in order to reduce noise introduced by the spatial differences between FS and FB. The resulting time dependent function is shown in Fig. 6. During the winter months, the stratification breaks down. For some reason, we get T_1 slightly cooler than T_5 during the winter, and so force $\partial T/\partial z = 0$ from April to August to avoid the upwelling term changing sign in winter. What causes this apparent inversion is not clear, it could be evidence of active heat loss in the upper 1 m

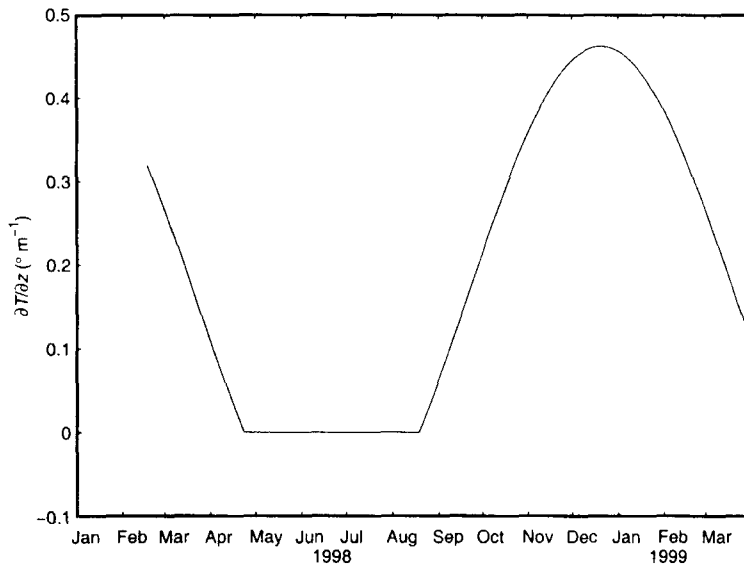


Fig. 6 Smoothed vertical thermal gradient, $\partial T/\partial z$, as used in the model (see text).

(the 1-m thermistors are mostly in the surf zone). Maximum stratification occurs in December, when $\partial T/\partial z$ reaches $0.45^\circ \text{ m}^{-1}$.

Parameters α and β were determined separately for 1 and 5 m depths by choosing them to obtain a “best-fit” between modelled and observed $\partial T/\partial t$. The best-fit criterion used here was to maximise mean coherence-squared between the two time series over the synoptic band. Coherence-squared is independent of the relative amplitudes of the time series, so this procedure produces only relative ratios α to β . For completeness, absolute values were then determined so that modelled and observed $\partial T/\partial t$ had the same energy in the synoptic band.

Temperature at 1 m is best fit by the model with $\alpha = 2.1 \times 10^{-6} \text{ m}^{-1}$; $\beta = 0$. Temperature at 5 m is best fit with $\alpha = 6.2 \times 10^{-7} \text{ m}^{-1}$; $\beta = 1 \times 10^{-5}$. At maximum stratification we obtain $\alpha/(\beta \partial T/\partial z) = 0.13$. It therefore appears that 1-m temperatures are unaffected by upwelling, whereas those at 5 m have an upwelling response. A physical interpretation of this is that because of the presence of a mixed layer at the surface, the vertical temperature gradient is zero, so that when upwelling or downwelling occurs, there is no associated temperature signal. At 5 m, however, there is sufficient stratification to allow upwelling to induce a temperature signal. It appears that in peak summer, upwelling at 5 m is c. 7 times more important than advection.

Figure 7 shows how well the model performs. In the left panels, we show coherence between $\partial T_1/\partial t$

and its predictor ($-\alpha U$) and in the right panels, we show the coherence between $\partial T_2/\partial t$ and its predictor:

$$(-\alpha U + \beta \frac{\partial T}{\partial z} U).$$

Because the model for $\partial T_1/\partial t$ is proportional to U , the coherence between $\partial T_1/\partial t$ and U is essentially the same as that between T_1 and U , except that the phase has been rotated by 90° (coherence is slightly increased because of numerical effects associated with the differentiation of T_1). This is, of course, what was expected, and the model does not much improve the skill of predicting T_1 , beyond getting the phase right.

At 5 m, however, skill using the model is increased over using the wind alone (compare Fig. 5B with Fig. 7B). Using the model increases both the coherence levels (especially in the 5–10-day band where coherence-squared doubles) and brings the phase close to zero.

DISCUSSION

Based on 1 year of data, coastal temperature from around Kaikoura Peninsula shows cooling events occurring mainly during the summer. These events contribute to variability within the synoptic band. In this band, temperature at both 1 and 5 m is coherent with the along-shore wind, but with different cross-spectral phase. At 5 m, the time-derivative of

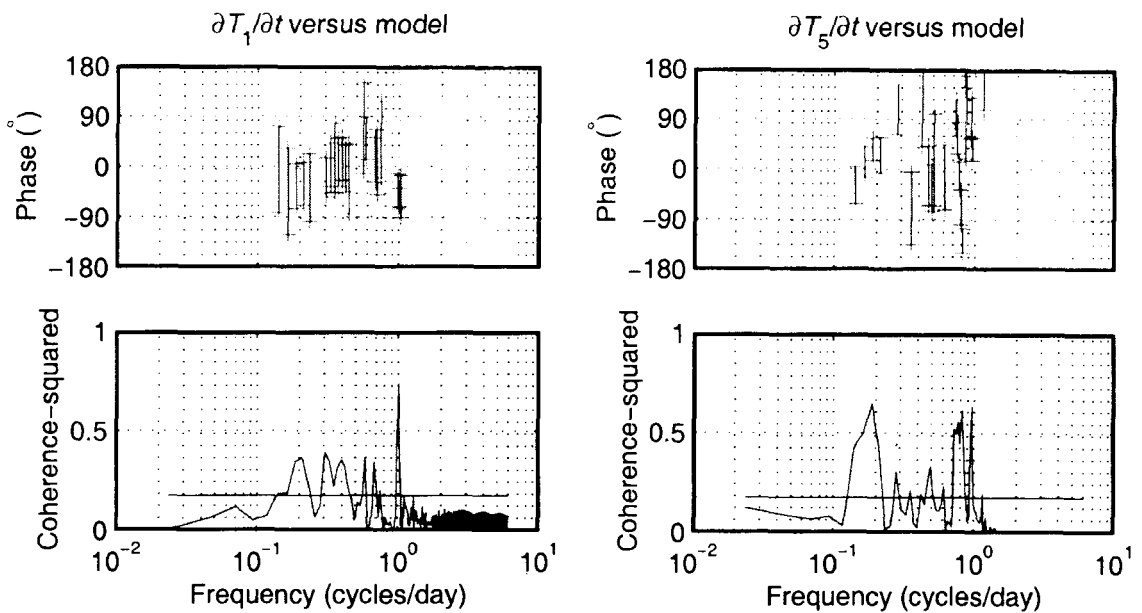


Fig. 7 Cross-spectra between time-derivative of temperature and model results (see text).

Left panels: cross-spectra between $\partial T_1/\partial t$ and $(-\alpha U)$. Right panels: cross-spectra between $\partial T_5/\partial t$ and $(-\alpha U + \beta \frac{\partial T}{\partial z} U)$.

temperature is in phase with the wind, whereas at 1 m, the time-derivative of temperature is out of phase with the wind.

The model introduced here produces a predictor that has along-shore advection and upwelling parameterised in terms of the along-shore wind velocity. This predictor has higher coherence with the time-derivative of temperature than does wind alone. At 1 m, the best-fit is obtained with the upwelling term set to zero. This intriguing result may be because the mixed-layer is deep enough so that temperature at 1 m sees little or no effect of upwelling. At 5 m, however, the thermocline is well enough developed during the summer so that upwelling produces a signal. Per unit wind speed, upwelling produces nearly an order of magnitude more temperature change than does along-shore advection.

However, along-shore advection and upwelling (or downwelling) are not the only processes that can affect coastal temperature. The results presented here are pertinent to the synoptic band only, but other processes including radiative heating, wind mixing, and tidal mixing which are generally more important at other time scales may also have some impact in the synoptic band. For example, although we do not

show it, temperature has a strong diurnal signal associated with radiative heating. The diurnal amplitude is about 1°C in summer, and it is modulated on timescales of days. While this modulation is probably because of changes in cloudiness associated with the passage of weather systems, we could find no coherence between it and the along-shore wind. This suggests that any linkage between along-shore wind and radiative cooling is complex, and thus unlikely to lead to the observations seen here.

Similarly, wind mixing leads to cooling at the surface and warming at the base of the thermocline. Under certain conditions wind mixing could reduce temperature at 1 m while increasing temperature at 5 m, and could thus lead to the 180° phase difference seen between 1 and 5 m. However, two factors point to this mechanism being unlikely for the observations made here. One is that such a mechanism would lead to the temperature signal being in phase—or out of phase—with wind stress, yet we find cross-spectral phase between T and U is c. 90° (Fig. 5). Also, since U routinely goes negative, we would expect a higher coherence between T and $|U|$ than with U . In fact coherence (not shown) reduces. We do not suggest that such a mechanism does not

exist, for example, strong northerly winds will lead to increased vertical mixing and will confound the advection-upwelling mechanism proposed here, but it seems they do not overcome it.

Tidal mixing, which in other regions can have a large impact on coastal temperatures can probably be safely excluded as a mechanism, because even though tides have some modulation in the synoptic band (e.g., the 14-day spring-neap cycle), these modulations will not be coherent with the local wind.

A simple model of the form used here omits considerable complexity in the dynamics. In particular, water mass variations are ignored, and the relationship between wind stress and along-shore current has been extremely simplified. The model also assumes that upwelling and downwelling are symmetric processes, but this is unlikely to be little better than a first approximation (de Szoeko & Richman 1981). Similarly, the use of the low-pass filtered vertical temperature gradient (Fig. 6) and the assumption of constant along-shore temperature gradient are only first approximations to reality. Incorporating variable $\partial T/\partial x$ and $\partial T/\partial z$ could increase the fits, but such parameter manipulation would not significantly affect the conclusions derived from the model.

We have not shown it explicitly here, but cross-spectra between the year-long records from the two most separated sites (FS1 and WW1) shows significant coherence at all time scales with zero phase difference. This suggests that the water masses impinging the peninsula are the same all along the coastline, and was the basis of the assumption of no spatial gradients around the peninsula that we had to make in order to develop the model. However, there are temperature differences between these sites, and this difference shows a seasonal signal. During summer FS1 gets up to 1°C warmer than WW1. Summer is also when the temperature difference shows largest synoptic band oscillations. We speculate that this reflects the more sheltered location of the Field Station site so that during periods of calm weather local heating leads to a warmer surface layer. During or after strong wind events, this local heating is either broken down by mixing or flushed away by advection.

Geographical variation of exposure to offshore events, combined with mechanisms such as this is probably why cooling events do not always have the same amplitude around the Kaikoura Peninsula. If this localised variability in the responses to upwelling and advection proves to be the true over

a longer time span, very localised events may determine differences in the biota among sites.

One cannot expect the model derived here to provide precise predictions of coastal temperature. Its main purpose is to explain the observed phase difference between 1 and 5 m, and between temperature and wind. It has provided an analysis of the different roles along-shore advection and upwelling play in determining coastal temperature variability. The importance of this study is that it helps direct future research into the region, particularly as it relates to the linkages between onshore and offshore events.

ACKNOWLEDGMENTS

We thank Robyn Dunmore and Dave Taylor for their efforts in deploying and maintaining the thermistor array under difficult conditions. We thank two anonymous reviewers for constructive comments. We acknowledge the support of the Foundation for Research, Science and Technology, Grant UOC610 and the logistic support provided by Jack van Berkel, and the University of Canterbury.

REFERENCES

- Andrew, N. L. 1988: Ecological aspects of the common sea urchin, *Evechinus chloroticus*, in northern New Zealand: a review. *New Zealand Journal of Marine and Freshwater Research* 22: 415–426.
- Chiswell, S. M. 1994: Variability in sea surface temperature around New Zealand from AVHRR images. *New Zealand Journal of Marine and Freshwater Research* 28: 179–192.
- Chiswell, S. M. 1996: Variability in the Southland Current, New Zealand. *New Zealand Journal of Marine and Freshwater Research* 30: 1–18.
- Creese, R. G. 1988: Ecology of molluscan grazers and their interactions with marine algae in north-eastern New Zealand: a review. *New Zealand Journal of Marine and Freshwater Research* 22: 427–444.
- de Szoeko, R. A.; Richman, J. G. 1981: The role of wind-generated mixing in coastal upwelling. *Journal of Physical Oceanography* 11: 1534–1547.
- Farrell, T. M.; Bracher, D.; Roughgarden, J. 1991: Cross-shelf transport causes recruitment to intertidal populations in central California. *Limnology and Oceanography* 36: 279–288.

- Gaines, S. D.; Roughgarden, J. 1985: Larval settlement rate: a leading determinant of structure in an ecological community of the marine intertidal zone. *Proceedings of the National Academy of Sciences* 82: 3707–3711.
- Harris, F. 1978: On the use of windows for harmonic analysis with the discrete Fourier transform. *Proceedings of the Institute of Electrical and Electronics Engineers* 66: 51–83.
- Heath, R. 1972: Oceanic upwelling produced by northerly winds on the north Canterbury coast, New Zealand. *New Zealand Journal of Marine and Freshwater Research* 6: 343–351.
- Heath, R. A. 1970: An occurrence of low water temperatures on the North Canterbury coast (note). *New Zealand Journal of Marine and Freshwater Research* 4: 223–226.
- Heath, R. A. 1975: Oceanic circulation and hydrology off the southern half of South Island, New Zealand: Wellington, *Memoir NZ Oceanographic Institute* 72. 36 p.
- Houtman, T. J. 1964: Surface temperature gradients at the Antarctic convergence. *New Zealand Journal of Geology and Geophysics* 7: 245–270.
- Jones, G. P. 1988: Ecology of rocky reef fish in northeastern New Zealand: a review. *New Zealand Journal of Marine and Freshwater Research* 22: 445–462.
- Menge, B. A. 1992: Community regulation: under what conditions are bottom-up factors important on rocky shores? *Ecology* 73: 755–765.
- Menge, B. A.; Daley, B. A.; Lubchenco, J. L.; Sanford, E.; Dahlhoff, E.; Halpin, P. M.; Hudson, G.; Burnaford, J. 1999: Top-down and bottom-up regulation of New Zealand rocky intertidal communities. *Ecological Monographs* 69: 297–330.
- Pond, S.; Pickard, G. L. 1978: Introductory dynamical oceanography. Oxford, Pergamon. 241 p.
- Ramage, D. L.; Schiel, D. R. 1999: Patch dynamics and response to disturbance of the seagrass *Zostera novaezelandica* on intertidal platforms in Southern New Zealand. *Marine Ecology Progress Series* 189: 275–288.
- Schiel, D. R. 1988: Algal interactions on shallow subtidal reefs in northern New Zealand: a review. *New Zealand Journal of Marine and Freshwater Research* 22: 481–489.
- Schiel, D. R.; Taylor, D. I. 1999: Effects of trampling on rocky intertidal algal assemblages in southern New Zealand. *Journal of Experimental Marine Biology and Ecology* 235: 213–235.
- Shaw, A. G. P.; Vennell, R. 1999: Variability of water masses through the Mernoo Saddle, South Island, New Zealand. *New Zealand Journal of Marine and Freshwater Research* 34: 103–116.
- Uddstrom, M. J.; Oien, N. A. 1999: On the use of high resolution satellite data to describe the spatial and temporal variability of sea surface temperatures in the New Zealand Region. *Journal of Geophysical Research* 104: 20729–20751.
- Underwood, A. J.; Fairweather, P. G. 1989: Supply-side ecology and benthic marine assemblages. *Trends in Ecology and Evolution* 4: 16–20.